

Reaction and bonding of Hf and Zr containing alloys to alumina and silica

Ronald E. Loehman*, Bryan D. Gauntt, F. Michael Hosking, Paul G. Kotula, Summer Rhodes, John J. Stephens

Sandia National Laboratories,¹ Albuquerque, NM 87185, USA

Abstract

We have investigated the wetting and reaction behavior of two less common transition element additives to braze alloys to learn more about their reaction and bonding mechanisms. Alloys of Ag with different amounts of Hf or Zr were reacted in a controlled atmosphere furnace with sapphire, alumina of 99.6 and 96% purity, and fused silica. We determined contact angles during heating and examined cross sections after cooling using electron analytical techniques. Different interfacial microstructures were obtained when the active metal was varied in an otherwise constant system. The Hf-containing alloys reacted with polycrystalline Al_2O_3 and had a dispersion of Hf-containing particles near the interface. If there were a reaction layer with the Al_2O_3 it was below the resolution of the analysis. By contrast, Zr reaction products were more evident and appeared to have diffused away from the interface into the alloy. The microstructural observations are interpreted using available thermodynamic data and known phase relations.

© 2003 Elsevier Ltd. All rights reserved.

Keywords: Al_2O_3 ; Bonding; MgO

1. Introduction

One of the most common methods for joining ceramics is the use of so-called active braze alloys that contain small concentrations of a transition element, such as Ti, V, or Zr, in an otherwise unreactive alloy.¹ The most widely used active braze alloy for ceramic joining is the 62 wt.%Ag–28 wt.% Cu eutectic composition with 1–4 wt.% Ti.² Braze alloys that contain active elements wet many ceramics when molten and adhere to them once cooled. Microscopic examination of the ceramic–braze alloy interface usually reveals evidence of reaction between the transition metal and the ceramic.^{3–8} Developing robust joining processes requires understanding how the reactions are influenced by materials and process variables such as alloy and ceramic compositions, temperature, reaction time, and furnace atmosphere.

In this paper we report the results of a study of reaction interfaces formed when Ag/Hf and Ag/Zr alloys were heated on a series of Al_2O_3 -based ceramics and fused silica. The selection of ceramics allowed us to test the effects of varying Al_2O_3 : SiO_2 ratios on the interfacial reactions. The Ag functions as an inert solvent for the transition metal, and by varying the Ag:transition metal ratio we could control the chemical activity of the active species. Based on a comparison of their Gibbs energies for oxidation, as presented in Table 1,⁹ one would expect Zr and Hf to behave similarly to Ti as an active constituent of braze alloys. That is, as an alloy constituent it would be expected to promote wetting and adhesion of the alloy to ceramic surfaces as a result of interfacial oxidation–reduction reactions.

2. Experimental

The alloys were made by arc melting mixtures of reagent grade Zr or Hf and Ag and casting them into ingots. The resulting alloys either were rolled into foil or were sliced into thin wafers with a band saw. The compositions are presented in Table 2.

* Corresponding author. Tel.: +1-505-272-7601; fax: +1-505-272-7304.

E-mail address: loehman@sandia.gov (R.E. Loehman).

¹ Sandia is a multiprogram laboratory operated by Sandia Corporation, a Lockheed Martin Company, for the US Department of Energy under Contract DE-AC04-94AL85000.

Table 1

Gibbs energies for oxide formation at 1300 K^o (ΔG_f^0 at 1300 K for $M + O_2 = MO_2$)

Oxide	ΔG_f^0 kJ/mol O ₂
VO ₂	−483.5
TiO ₂	−707.7
ZrO ₂	−854.5
HfO ₂	−909.1

Table 2

Chemical compositions of Zr–Ag and Hf–Ag alloys

Active element	Weight%	Atomic%
Zr	2	2.4
Hf	2.5, 3.4 and 6.8	1.5, 2.1 and 4.2

The substrates were four commercial ceramics, which were used with their as-received surface finishes.

1. Sapphire (optical grade);
2. 99.6% alumina, balance Ca, Mg silicate glass (Coors Ceramics Co. electronic substrates);
3. 96% alumina, balance Ca, Mg silicate glass (Coors Ceramics Co. electronic substrates); and
4. Fused silica (optical polish).

The substrates were cleaned in methanol, dilute hot detergent solution, deionized water, and then dried in air. The alloy specimens were placed on top of the ceramics in an atmosphere-controlled furnace for the reaction experiments. Some experiments used a sandwich geometry where the alloy was heated between two ceramic pieces of the same composition. Enough alloy was used to give a metal thickness of 2–3 mm. The furnace was heated by a tubular, graphite resistance element contained in a water-cooled, stainless steel vacuum chamber. The specimens were isolated from the heating element by a coaxial ceramic tube that was sealed by o-rings in the end flanges. Quartz windows in each flange allowed the sample to be observed during heating. All the runs were conducted in flowing Ar that had been passed through a Ti–Zr getter held at 800 °C. The specimens were heated to 1100 °C at 20°/min and held for either 5 or 30 min and then cooled to room temperature at 20 °C/min. The Ag/Hf alloys were tested on all the listed ceramics; the Ag/Zr alloy was tested only on the Al₂O₃ ceramics. The contact angle of the molten metal on the ceramic was measured with a telegoniometer at the end of the time at 1100 °C. The cooled specimens were cut perpendicular to the ceramic–metal interface, polished down to a 1 µm finish with diamond paste and then examined in a scanning electron microscope (SEM) equipped with an energy dispersive spectrometer (EDS).

3. Results

All the Ag/Hf and Ag/Zr alloys melted at 1100 °C and wet each of the ceramic substrates. The Ag/Hf alloys that were heated for only 5 min separated from the ceramics after cooling. Those ceramics were discolored where the metal had been in contact, indicating there might have been some reaction at the periphery of the drop, but if there were any reaction it was insufficient to bond the alloy to the ceramic. By contrast, all the Ag/Zr specimens and the Ag/Hf specimens heated for 30 min stuck to the ceramic substrates.

3.1. Ag/Hf Alloys

SEM examination of cross sections of Ag/Hf alloys heated on the 96 and 99.6% alumina showed they had similar microstructures. Cross sections for all the alloys revealed a broad dispersion of small particles of about 1 µm in diameter near the Al₂O₃ interface, as shown in Fig. 1 for a specimen of Ag/2.5 wt.%Hf heated between pieces of 99.6% alumina for 30 min at 1100 °C. As can be seen in Fig. 1, both the upper and lower interfaces have the same array of fine, bright particles, whereas they are absent in the center. Distributions of the fine particles were similar for the other Ag/Hf alloys on both the 96 and 99.6% alumina substrates.

There also was a region of larger particles of about 20 µm diameter that appears only at the bottom interface of both the sandwich and open face geometries. The concentration of those larger particles increased with the amount of Hf in the alloy and was particularly evident with the Ag/6.8%Hf composition. Fig. 2 shows this result for an Ag/6.8%Hf specimen heated on 99.6% alumina for 30 min at 1100 °C. Both sizes of particles appear in bright contrast when imaged in the back-scattered electron mode, indicating they had a higher atomic number than the matrix. EDS analysis of the particles gave peaks only for Hf and Ag. Because the fine particles were smaller than the diameter of the spot excited by the electron beam in the EDS analysis, it is impossible to determine if the Ag signal was all from the matrix or if the particles themselves contained some Ag.

Examination of alloy–Al₂O₃ interfaces revealed little evidence for reaction, as illustrated in Fig. 3 for an Ag/2.5 wt.%Hf specimen heated on 96% alumina for 30 min at 1100 °C. Some samples had a few isolated regions along the interface that were approximately 1 µm thick and that, according to EDS analysis, contained Hf, O, and some Ag (possibly signal from the surrounding matrix).

Cross sections of Ag/Hf alloys heated on SiO₂ at 1100 °C had a more-or-less continuous layer a few micrometers thick at the interface, as illustrated in Fig. 4a. EDS analysis showed that phase contained Hf and O, suggesting that it was the product of reaction between Hf and the SiO₂. Apart from the interfacial

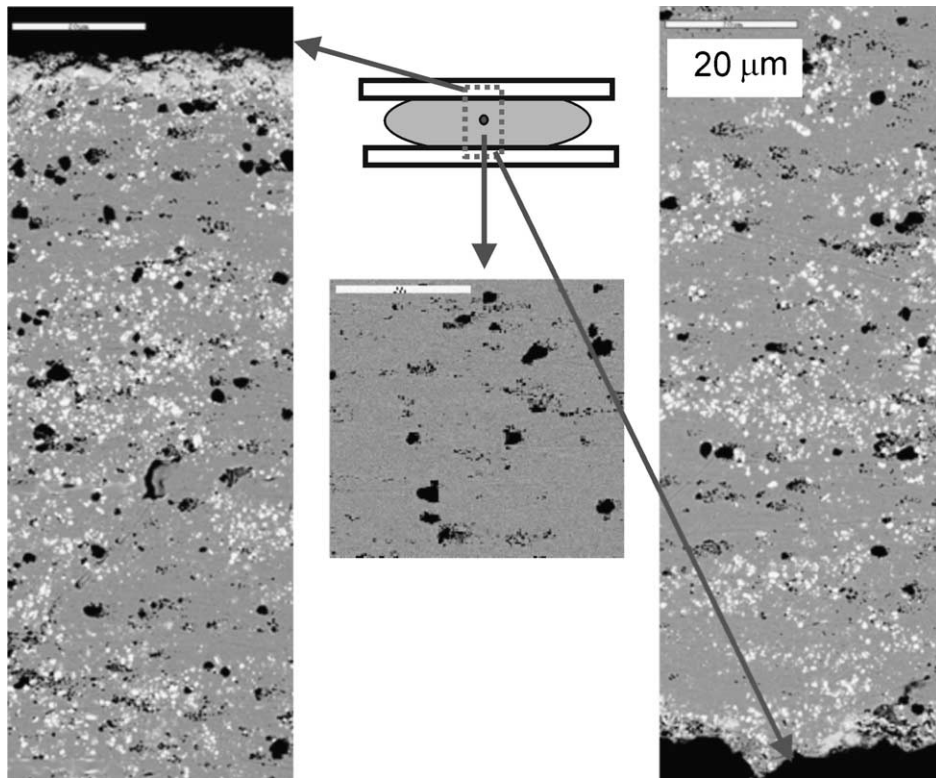


Fig. 1. Composite of SEM scan across structure resulting from heating Ag/2.5 wt.%Hf between two pieces of 96% Al_2O_3 . The specimen was at 1100 °C for 30 min.

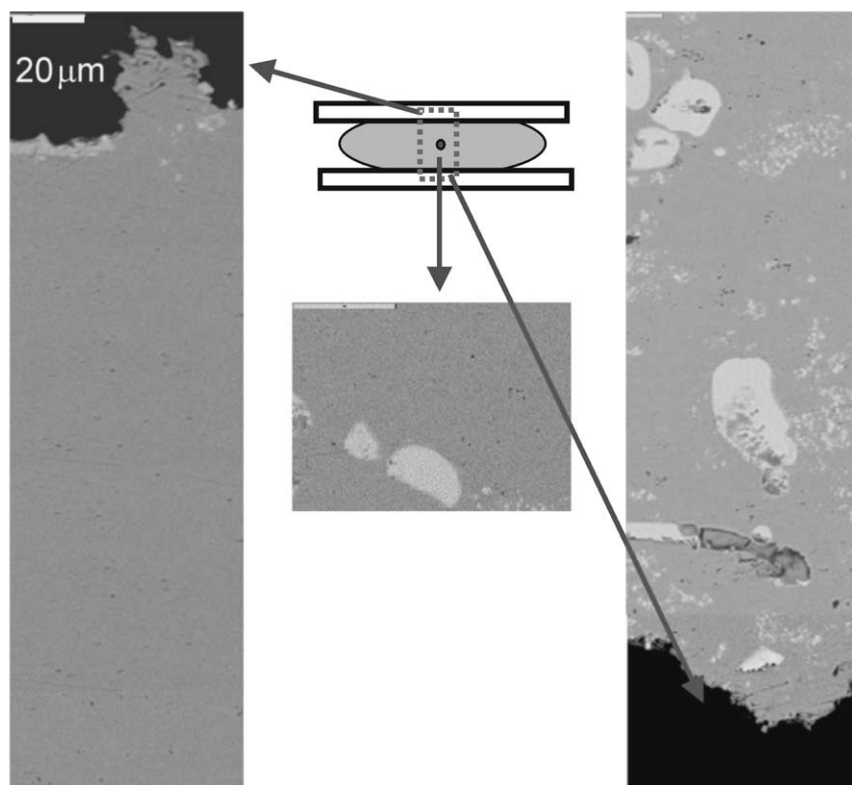


Fig. 2. Composite of SEM scan across structure resulting from heating Ag/6.8 wt.%Hf between two pieces of 99.6% Al_2O_3 . The large Hf-containing particles are found only at the lower interface. The specimen was at 1100 °C for 30 min.

layer, the microstructures of the alloys heated on SiO_2 were similar to the ones on Al_2O_3 in that they had the same dispersion of fine Hf-containing particles in the alloy and the larger, 10–20 μm particles near the lower interface. As shown in Fig. 4b, the larger particles were more prevalent in the alloys with more Hf, similar to the case with the alumina substrates. The thickness of the interfacial layer did not vary much with Hf concentration, which can be seen by comparing Fig. 4a and b.

The contact angles of the molten Ag/Hf alloys on the ceramic substrates varied with both the Hf content of the alloy and the amount of SiO_2 in the ceramic. Fig. 5 is a plot of contact angle of the three alloys after 30 min at 1100 °C as a function of SiO_2 content in the ceramic, assuming all the grain boundary phase in the alumina specimens is SiO_2 . That assumption is not strictly true, since the alumina second phases also contain small amounts of other oxides such as MgO, CaO, and Al_2O_3 . However, even if we knew the absolute SiO_2 content it would change the shapes of the curves only slightly and not affect the observed trends. One of those trends, as shown in Fig. 5, is that the contact angle decreases with increasing amount of SiO_2 in the ceramic, as would be expected in a system exhibiting reactive wetting. However, the contact angles on a given substrate increase with increasing Hf concentration, which is contrary to what one would expect if wetting were driven by reaction between Hf and SiO_2 .

3.2. Ag/Zr Alloy

As stated above, the Ag/2%Zr alloy wet all the Al_2O_3 ceramics and adhered to them after cooling, even for heating times of only 5 min at 1100 °C. The contact angle for the Ag/2 wt.%Zr alloy at 1100 °C was less than that of any of the Ag/Hf alloys for all three of the alumina ceramics. The general appearance of the

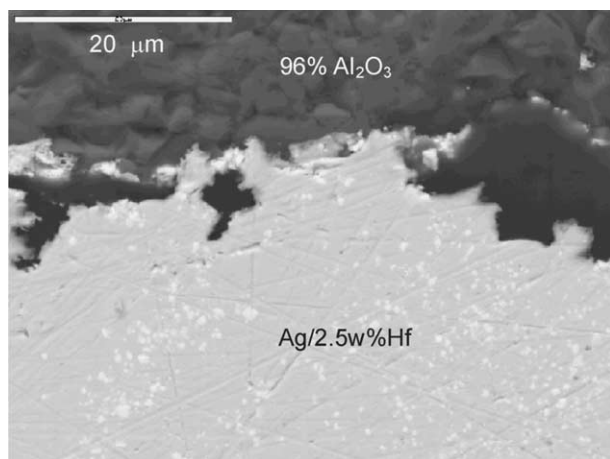
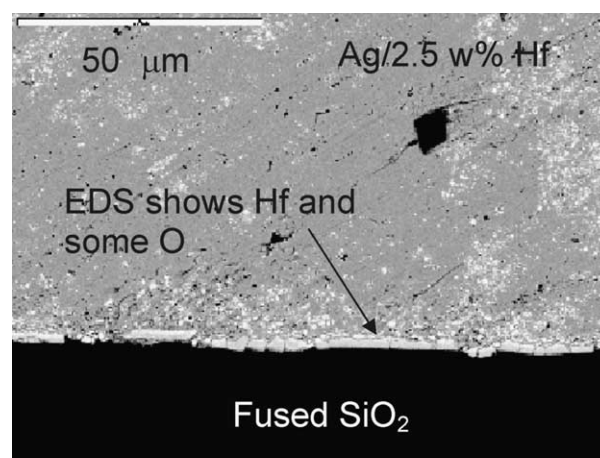
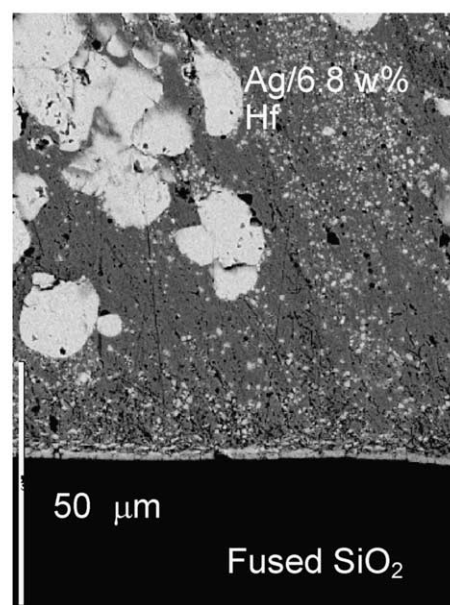


Fig. 3. Little or no reaction zone is observed after heating Ag/2.5 wt.%Hf on 96% alumina for 30 min at 1100 °C. EDS analysis shows the small bright particles are mostly Hf.

Ag/Zr– Al_2O_3 interface is shown in Fig. 6, which is a cross section prepared by the focused ion beam milling (FIB) technique. Zr appears to react more extensively with the alumina ceramics than does Hf, as shown in Fig. 7, where an interfacial zone about 20 μm thick is observed between the 99.6% alumina ceramic and the Ag/2%Zr alloy. At least two phases are apparent in the interfacial region, as indicated by the results of EDS analysis of different parts of the interface that are also shown in Fig. 7. The bright phase near the unreacted alumina at the bottom of the figure contains Ag, some Zr, and possibly a trace of O, although the oxygen could have been from overlap of the probe with the Al_2O_3 ceramic. The dark phase that makes up a majority of the reaction zone contains Zr, some O and a trace of



(a)



(b)

Fig. 4. (a): Interface after heating Ag/2.5 wt.%Hf on fused silica for 30 min at 1100 °C. (b): Interface resulting from heating Ag/6.8 wt.%Hf on fused silica for 30 min at 1100 °C. EDS analysis shows the large bright particles in the alloy contain mostly Hf.

Ag. The bright phase away from the interface contains Ag and Zr in approximately equal amounts with a trace of O.

Fig. 8 is a cross section of Ag/2%Zr heated on 96% alumina for 30 min at 1100 °C. The microstructure is similar to that shown in Fig. 7 for the 99.6% alumina, except that it shows more clearly that the Zr-containing reaction product has moved away from the interface and that next to the alumina there is a lot of Ag that contains some dissolved Al.

4. Discussion

Any explanation of Hf-ceramic reaction mechanisms must account for the two sizes of Hf-containing particles and their observed locations in the reaction cross sections. The microstructures illustrated in Figs. 1 and 2 are consistent with a two-stage segregation of Hf to the ceramic interface during heating. The larger particles are found only at the bottom interface and there are more of them when there is more Hf in the alloy. The Ag–Hf phase diagram is not available, so the solidification paths of the Ag/Hf alloys cannot be inferred from literature data. However, the observed microstructures suggest the larger particles are Hf or a Hf-containing phase that exceeds some solubility limit and which nucleates initially in the molten alloy and then grows during the 1100 °C heating period. The particles would sink in the molten alloy toward the lower interface because Hf ($\rho = 13.6 \text{ g/cm}^3$) is denser than Ag ($\rho = 10.5 \text{ g/cm}^3$). The smaller particles are concentrated at both interfaces in experiments with the sandwich geometry, which suggests they precipitate only during cooling and therefore have less time to grow and settle before everything solidifies. The concentration of Hf toward the alumina and silica

interfaces implies there is a chemical driving force for segregation of Hf to the ceramic–metal interface.

Based on some of our prior work¹⁰ we do not believe that either type of Hf-containing particle is HfO_2 , as would be expected from the oxidation–reduction reaction $3\text{Hf} + 2\text{Al}_2\text{O}_3 \rightarrow 3\text{HfO}_2 + 4\text{Al}$. That reaction is feasible with a $\Delta G^\circ = -217.9 \text{ kJ}$ at 1400 K.⁹ However, the microstructure of the HfO_2 reaction product found in the earlier study¹⁰ when we heated 60Ag–40Cu–1Hf (at.%) on 99.6% Al_2O_3 at 1000 °C was totally different from the present observations. In the earlier work the HfO_2 product was found by transmission electron microscopic (TEM) examination to be a layer of 20–40 nm particles with equiaxed geometry that were embedded in the Al_2O_3 grains along the alloy interface. The small HfO_2 particles, which were confirmed as such by electron diffraction measurements, had clearly grown into the Al_2O_3 grains during reaction. Although the Ag/Cu/Hf and Ag/Hf alloy compositions are different, neither Ag nor Ag/Cu is an active participant in any interfacial reaction so we would expect the microstructure of the HfO_2 products to be similar for the two alloys. We have not yet done TEM analysis of the present specimens so we do not know whether they contain fine scale HfO_2 precipitates similar to those seen in the earlier study. However, it is reasonable to assume that any HfO_2 reaction product layer will be thin and tightly adhered to the Al_2O_3 interface.

The microstructures resulting from reaction of the Ag/Hf alloys with SiO_2 contain both types of Hf-containing particles observed in the Ag/Hf– Al_2O_3 cross sections. However the Ag/Hf– SiO_2 cross sections also show a more-or-less continuous reaction layer next to the ceramic that is a few micrometers thick and that

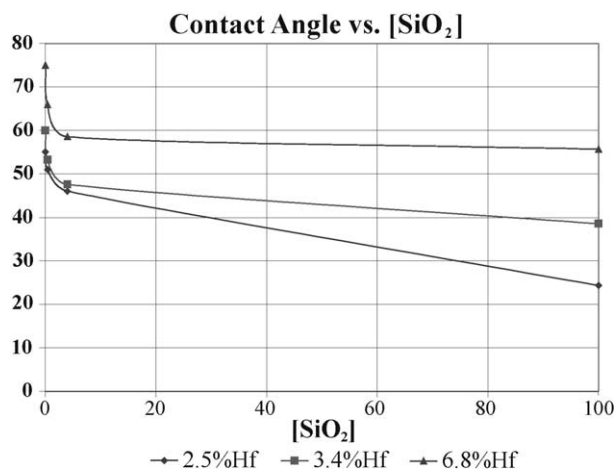


Fig. 5. Wetting angles for three Ag/Hf alloys after heating on sapphire, 99.6% alumina, 99.6% alumina, and fused silica for 30 min at 1100 °C. The atmosphere was gettered Ar.

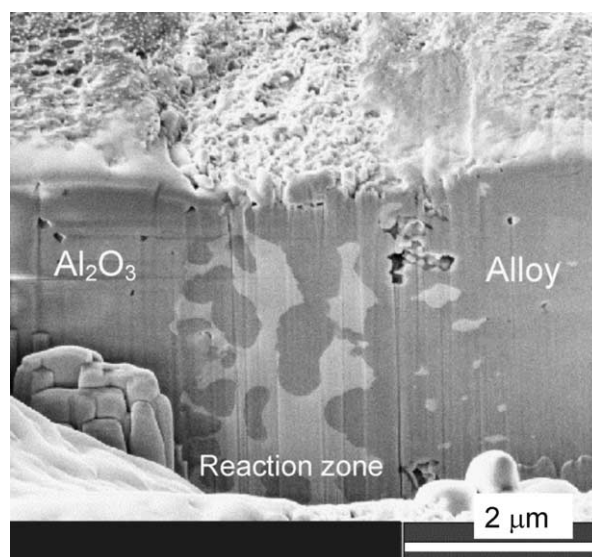


Fig. 6. Cross section of interface from heating Ag/2 wt.%Zr on 99.6% alumina for 30 min at 1100 °C. The specimen was prepared by the focused ion beam (FIB) milling technique.

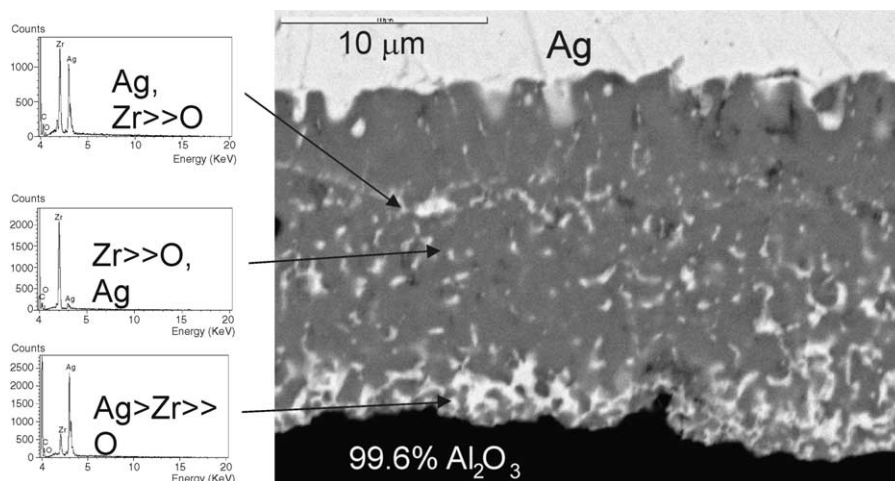


Fig. 7. Zr concentrates and reacts at interface after heating Ag/2 wt.%Zr between 99.6% alumina substrates.

according to EDS analysis contains only Hf and O. That result suggests the layer next to the ceramic is HfO_2 , which would form according to $\text{Hf} + \text{SiO}_2 \rightarrow \text{HfO}_2 + [\text{Si}]_{\text{Ag}}$, where the square brackets indicate molar concentration and $[\text{Si}]_{\text{Ag}}$ indicates Si dissolved in the Ag alloy. The ΔG° for that reaction, neglecting the heat of solution of Si in Ag, is favorable and is -232.6 kJ at 1400K (9). A comparison of the Gibbs energies for reaction of Hf and Al_2O_3 with Hf and SiO_2 shows that, when normalized to 1 mole of HfO_2 product, the latter reaction is greater than three times more negative than the former ($\text{Hf} + \text{Al}_2\text{O}_3$, $\Delta G^\circ = -72.6$ kJ at 1400 K; $\text{Hf} + \text{SiO}_2$, $\Delta G^\circ = -232.6$ kJ at 1400 K). Thus, the oxidation–reduction reaction between Hf and SiO_2 is significantly more favorable than reaction between Hf and Al_2O_3 . This difference in ΔG° s could account for the more extensive reaction between Ag/Hf and SiO_2 than with Al_2O_3 .

The trends in wetting angles shown in Fig. 5 are influenced by two effects. The first effect is chemical. That is, the decrease in contact angle with $[\text{SiO}_2]$ for constant $[\text{Hf}]$ is similar to that observed with other systems that exhibit reactive wetting; i.e. the greater the concentration of reactants, the lower the contact angle.^{5,8,11} The second effect is mechanical. The increase in wetting angle on a given ceramic when $[\text{Hf}]$ in the alloy is increased is explained by the larger number of solid Hf particles at the molten alloy–ceramic interface. If, as argued here, those large solid particles were present soon after the alloy melts on the ceramic, they would tend to inhibit flow and spreading, strictly as a mechanical effect. Thus, the wetting angles would increase, as observed, when a larger $[\text{Hf}]$ in the alloy creates more solid particles at the interface.

The Ag/2 wt.%Zr alloy is the binary eutectic composition with a liquidus temperature of 940 °C.¹² Below

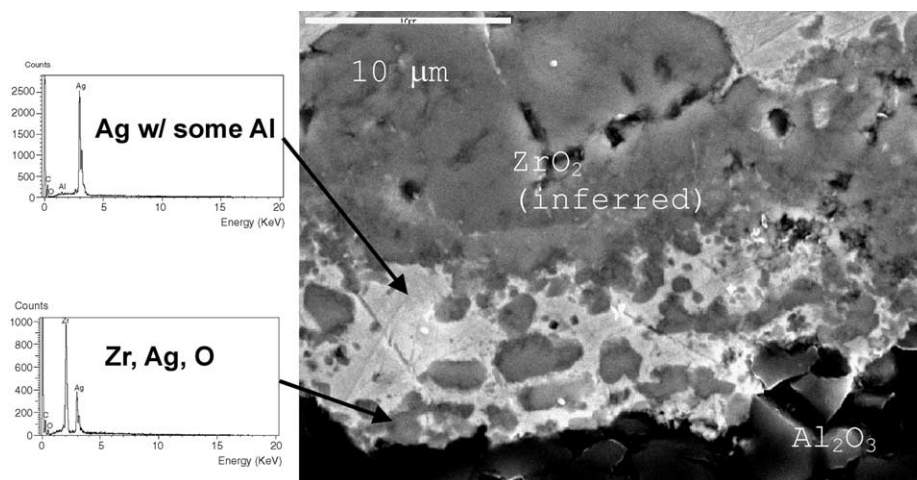


Fig. 8. Interface from Ag/2wt.%Zr on 96% alumina for 30 min at 1100 °C. ZrO_2 reaction product is inferred from EDS results and thermodynamic relations.

940 °C, Ag is in equilibrium with an AgZr phase according to the phase diagram.¹² None of the alloy microstructures observed in the Ag/2%Zr cross sections appeared to be the result of cooling of an Ag–Zr eutectic composition. Instead, all the Zr detected by EDS was segregated near the Al₂O₃ interface, as shown in Figs. 7 and 8. The layer is not continuous, as shown in Fig. 8, and there are extensive regions where the Zr-containing phase is separated from the interface by a phase with the same composition as the Ag matrix. The microstructure of the Ag/Zr–ceramic interfaces suggests a reaction sequence with three steps: (1) diffusion of Zr to the interface; (2) reaction between the Zr and Al₂O₃; and (3) diffusion of the product away from the interface.

The present results make only a circumstantial case for ZrO₂ as the reaction product in the Ag/Zr–Al₂O₃ wetting experiments. Reaction of Zr with Al₂O₃ is thermodynamically favorable, with a $\Delta G^\circ(1400\text{ K}) = -49.9\text{ kJ}$ for $3\text{Zr} + 2\text{Al}_2\text{O}_3 \rightarrow 3\text{ZrO}_2 + 4\text{Al}$.⁹ The EDS data for the Zr-containing phases in Figs. 7 and 8 indicate some oxygen, but the signal is weak, possibly from absorption of the oxygen X-rays by the surrounding Zr. TEM electron diffraction experiments that could resolve the issue are underway, but they have not been completed.

On the basis of thermodynamic driving force alone, one would expect more extensive reaction between Ag/Hf and Al₂O₃ ($\Delta G^\circ = -217.9\text{ kJ}$ at 1400 K) than between Ag/Zr and Al₂O₃ ($\Delta G^\circ = -49.9\text{ kJ}$ at 1400 K).⁹ However the results of the present work are opposite to that expectation. One possible explanation is that the alloys behave as non-ideal solutions; that is, the activities of the Hf and Zr in the Ag are different from their concentrations. Another explanation that has some support from the microstructural results is that, although the Hf–Al₂O₃ reaction is more favored thermodynamically, its kinetics appear slower than those for reaction between Zr and Al₂O₃. The HfO₂ reaction product observed in the Ag–Cu–Hf experiments¹⁰ was thin and tightly embedded in the Al₂O₃ grains at the interface. The reaction rate would be controlled by the rate of diffusion through the product layer. By contrast, the Ag/Zr reaction product in the present experiments has diffused away from the interface. The reaction rate in the Ag/Zr–Al₂O₃ experiments would be controlled by diffusion through the liquid alloy, which would be much faster than with the solid HfO₂ layer.

5. Conclusions

We have shown some substantial differences in the wetting and reaction behavior of Ag/Zr and Ag/Hf alloys on alumina and silica ceramics that seem to be

related to interfacial redox reactions. The Ag/Zr alloy has a lower contact angle and thicker reaction zone on alumina than Ag/Hf, although the thermodynamic calculations predict opposite behavior. We argue that, although Hf–Al₂O₃ reaction might have a higher driving force than reaction between Zr and Al₂O₃, the kinetics of the Hf–Al₂O₃ reaction are slowed by a diffusion barrier of HfO₂ product. The present results with the Ag/Hf alloys are not sufficiently detailed to reveal a reaction layer that we expect, based on prior work, to be only a few tens of nanometers thick. TEM analyses of the Ag/Hf and Ag/Zr reactions are underway and they should allow us to determine whether our assumed reaction mechanisms are correct.

One practical conclusion of this study is that both alloy systems may be useful for ceramic joining. Also, the observed differences in Zr and Hf behavior may allow the interfaces in joined ceramics to be tailored for specific properties. For example, Ag/Hf may be more useful when a very thin reaction layer is desired, but Ag/Zr would be more appropriate where a thicker composite interfacial layer would be useful.

References

1. Watkins, R. D., *Types of Joining and Their Uses. Engineered Materials Handbook*. ASM International, Materials Park, OH, 1991.
2. Mizuhara, H. and Oyama, T., *Ceramic/Metal Seals. Engineered Materials Handbook*. ASM International, Materials Park, OH, 1991.
3. Nicholas, M. G. and Mortimer, D. A., Ceramic/metal joining for structural applications. *Mater. Sci. Tech.*, 1985, **1**(9), 657–665.
4. Suganuma, K., Miyamoto, Y. and Koizume, M., Joining of Ceramics and Metals. *Ann. Rev. Mater. Sci.*, 1988, **18**, 33–47.
5. Loehman, R. E. and Tomsia, A. P., Joining of ceramics. *Am. Ceram. Soc. Bull.*, 1988, **67**(2), 375–380.
6. Elssner, G. and Petzow, G., Metal/Ceramic Joining. *ISIJ Int.*, 1990, **30**(12), 1011–1032.
7. Nicholas, M. G., *Joining of Ceramics*, 1st ed., Published on behalf of the Institute of Ceramics by Chapman and Hall, London, New York, 1990.
8. Pask, J. A. and Tomsia, A. P., *Wetting, Surface Energies, Adhesion, and Interface Reaction Thermodynamics, Engineered Materials Handbook*. ASM International, Materials Park, OH, 1991.
9. Robie, R. A., Hemingway, B. S. and Fisher, J. R., *Thermodynamic Properties of Minerals and Related Substances at 298.15K and 1 Bar Pressure and at Higher Temperatures, US Geological Survey Bulletin 1452*. US Govt. Printing Office, Washington, DC, 1979.
10. Loehman, R. E., and Kotula, P. G. Spectral imaging analysis of interfacial reactions and microstructure in brazing of alumina by a Hf–Ag–Cu Alloy. *J. Am. Ceram. Soc.* (in press).
11. Naidich, J. V., The wettability of solids by liquid metals. In *Progress in Surface and Membrane Science*, ed. D. A. Cadenhead and J. F. Danielli. Academic Press, London, 1981, pp. 353–484.
12. Massalski, T. B. and Okamoto, H., *Binary Alloy Phase Diagrams*, 2nd ed. ASM International, Materials Park, Ohio, 1990.